Supporting information

Dual-surfactant-capped Ag nanoparticles as a highly selective and sensitive colorimetric sensor for citrate detection

Samy M. Shaban[a,b], Jun Young Lee*[a], Dong-Hwan Kim[a,b]*,

[a]School of Chemical Engineering, Sungkyunkwan University, 16419, Republic of Korea

[b]Biomedical Institute for Convergence at SKKU (BICS), Sungkyunkwan University, 16419, Republic of Korea

*Email: dhkim1@skku.edu

1. Structure confirmation of GFEO surfactant

The chemical structure of the synthesized G surfactant was confirmed by FTIR and ^{1}H-NMR spectroscopy, as outlined in Figures S1a and S1b, respectively. Figure S1a shows the FTIR spectra of the GFEO surfactant, with loss of both hydroxyl and carbonyl groups related to carboxylic acid and appearance of a new band at 1733 cm^{-1} corresponding to carbonyl ester. Bands at 3012, 2920, 2871, 1456, and 1350 cm^{-1} correspond to aromatic protons, aliphatic asymmetric and symmetric –C–H, CH_2 bending, and CH_3 bending, respectively. The bands at 1610-1514 refer to C=C double bonds, while that in the range of 1100-1200 refers to the C–O ether group of ethylene oxide.

Number and distribution of protons in the synthesized GFEO surfactant were confirmed by ^{1}H-NMR spectra, as outlined in Figure S1b. The ^{1}H-NMR spectra of the GFEO surfactant shows the following signals: δ= 0.85 (t,6H, **2CH_3** alkyl chain); δ= 1.25 (m,32H, — 2 $COCH_2CH_2$**$(CH_2)_8$**CH_3), δ= 1.48 (m,4H, $2COCH_2$**CH_2**$(CH_2)_8CH_3$); δ= 2.19 (m,4H, 2CO**CH_2**$CH_2(CH_2)_8CH_3$); δ= 2.55 (m,4H, 2 –Ph-CH_2**CH_2**COO-), δ= 2.74 (m,4H, 2 –Ph-**CH_2**CH_2COO-); δ= 3.37-3.57 (m,272H, poly ethylene oxide group); δ= 4.56 (s,2H, -C**H**=C**H**-); δ= 6.6 (d,4H, meta-aromatic protons); and δ= 7 (d,4H, ortho-aromatic protons).

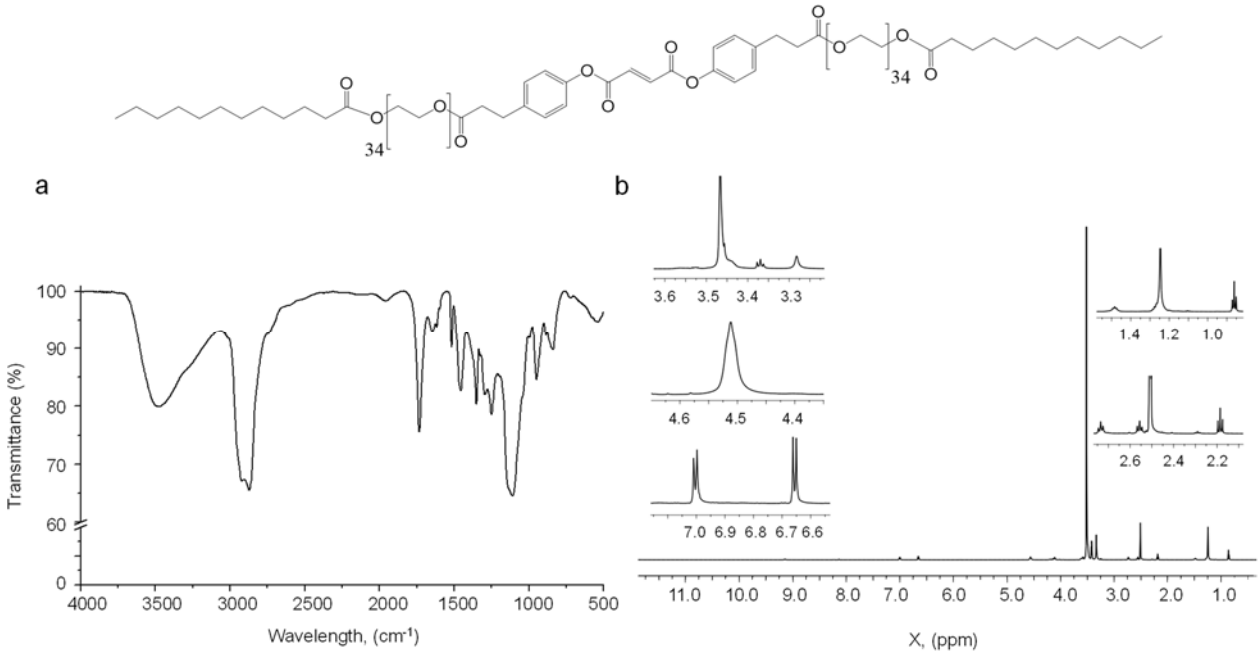

Figure S1. (a) FTIR and (b) ^{1}H-NMR spectra of the prepared GFEO surfactant.

2. Mechanism of citrate detection

The possible mechanism of citrate detection with the prepared Dual-AgNP sensor is a result of induced aggregation, as shown in the TEM images (Figures S2a & S2b) and the DLS measurements (Figures S3a & S3b).

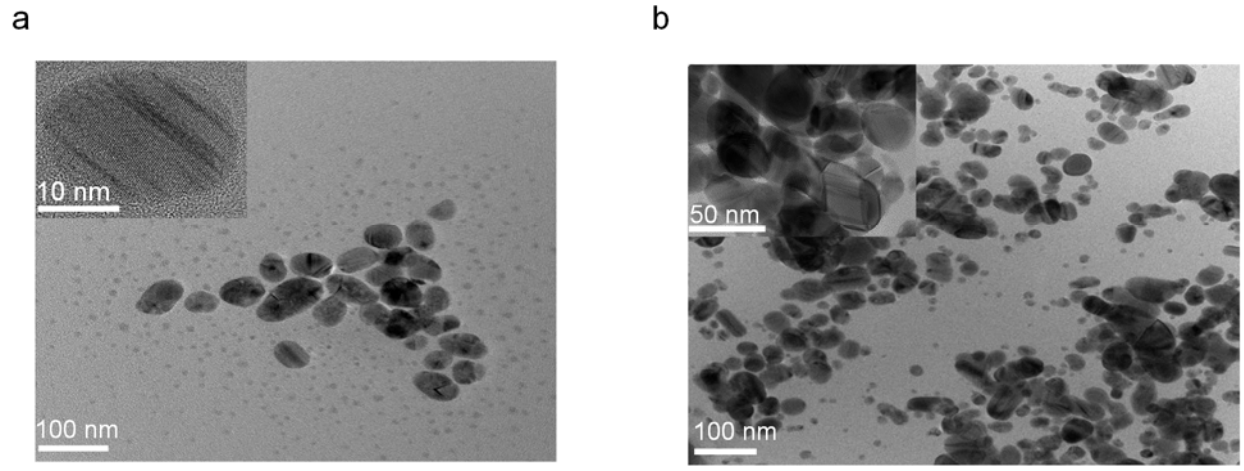

Figure S2. TEM images of the prepared Dual-AgNP sensor (a) before and (b) after incubation with citrate anion (130 µM).

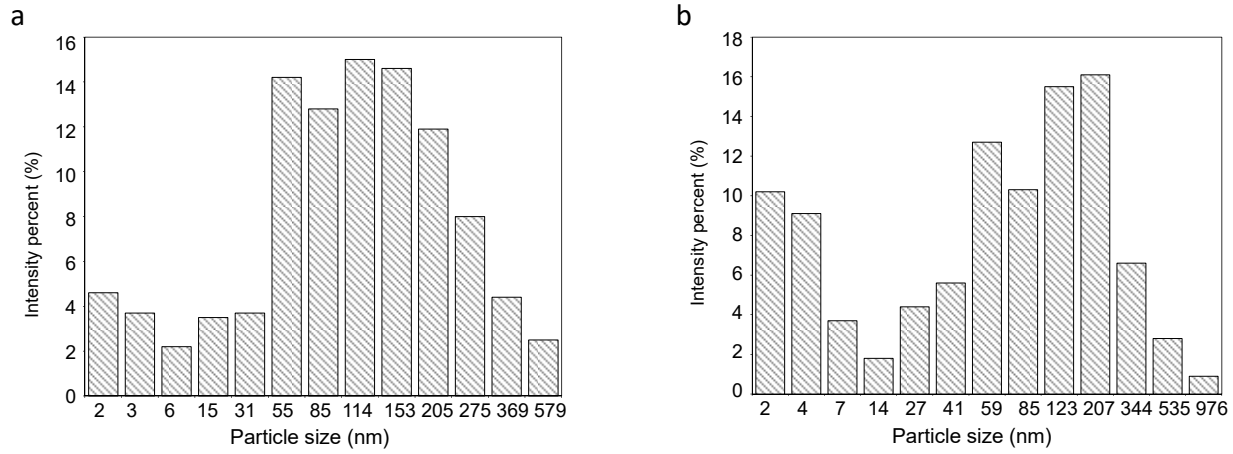

Figure S3. Size distribution of the obtained Ag nanoparticles in the synthesized Dual-AgNP sensor based on mixed surfactant (a) without citrate and (b) with 130 µM citrate.

3. Selectivity of mono-surfactant-capped AgNPs

The selectivity of mono-surfactant-capped AgNPs (i.e., CTAB-AgNPs and GFEO-AgNPs) toward various metal ions was investigated by UV-vis spectroscopy. Figures S4a and S4b show UV-vis spectra for interactions of mono-surfactant-capped AgNPs with various metal cations. The series of metal ions tested in the present study did not show any significant interaction with the mono-surfactant-capped AgNPs.

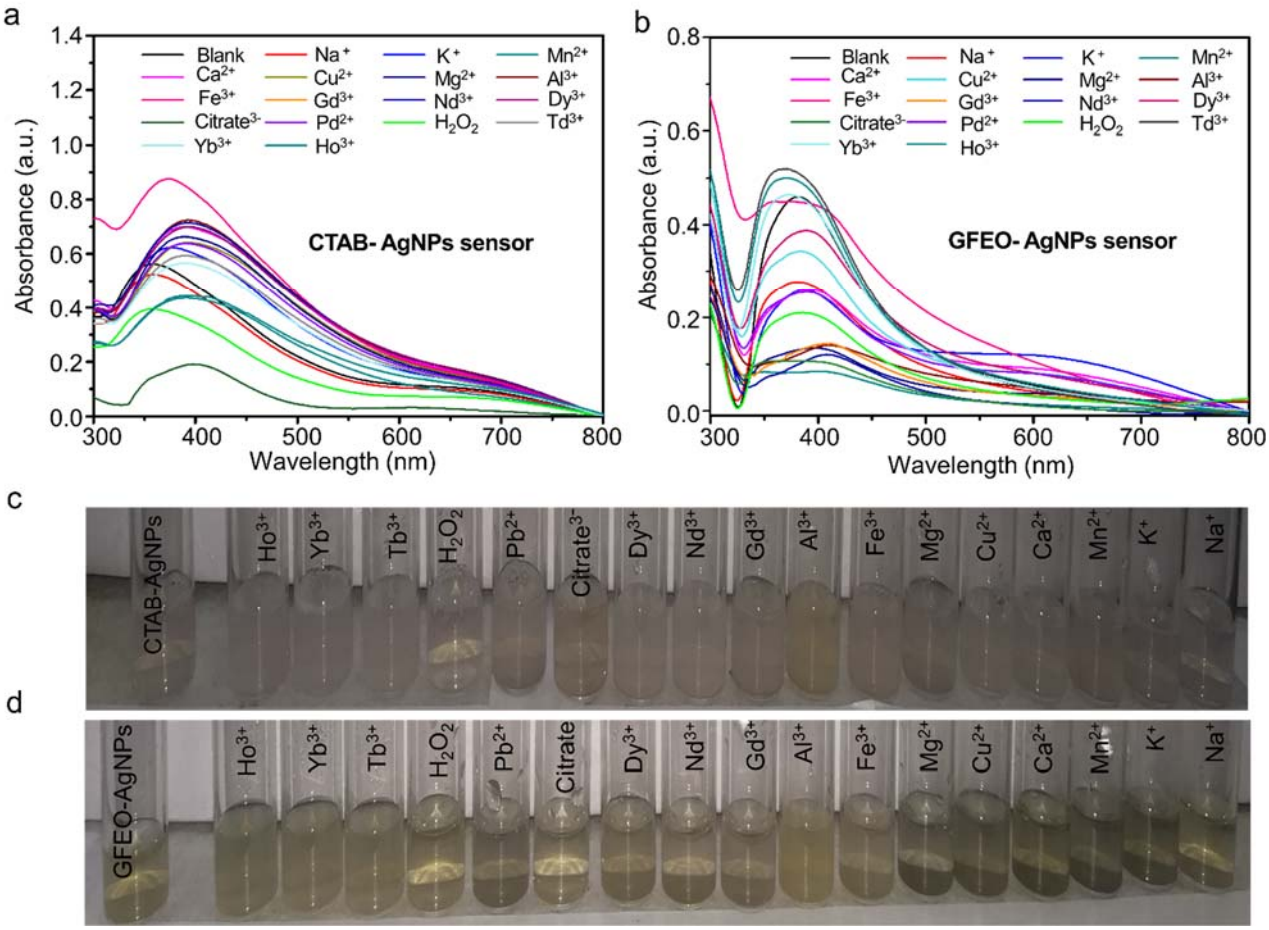

Figure S4. UV-vis spectra of (a) CTAB-AgNP sensor and (b) GFEO-AgNP sensor interacting with various metal cations (concentration of 200 μM). Photographs of the (c) CTAB-AgNPs and (d) GFEO-AgNPs.

4. Dual-AgNP sensor optimization

Optimization of the sensor was conducted by diluting the prepared Dual-AgNP sensor two, four, eight, and ten times to produce diluted Dual-AgNPs-2X, Dual-AgNPs-4X, Dual-AgNPs-8X and Dual-AgNPs-10X, respectively. Their responses toward citrate detection are outlined in Figure S5.

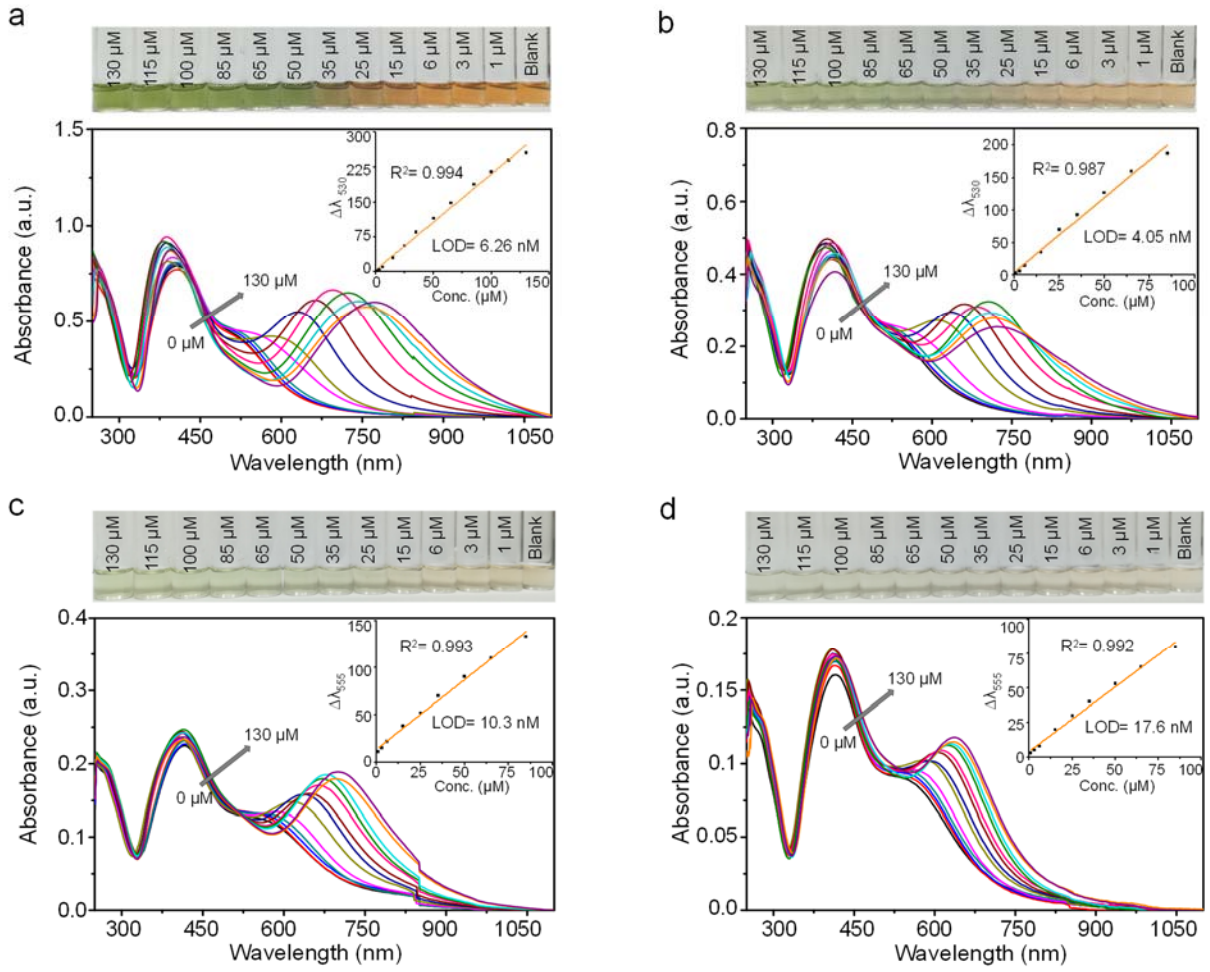

Figure S5. UV-vis spectra of the diluted Dual-AgNP solutions after adding different concentrations of citrate: (a) Dual-AgNPs-2X, (b) Dual-AgNPs-4X, (c) Dual-AgNPs-8X, and (d) Dual-AgNPs-10X. In each case, the inset curve is the corresponding calibration curve.

5. Visual detection of citrate by the fabricated paper-based analytical device.

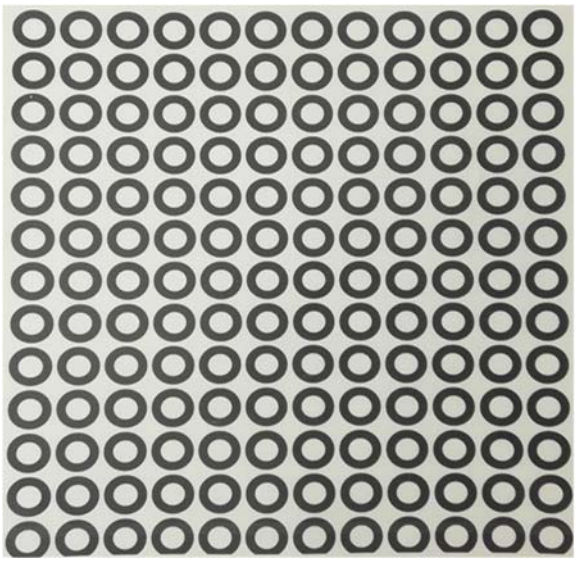

Figure S6. Photo of paper sheet after creating hydrophilic zones by laser printing with waxy ink.